Propaedeutic study for the delivery of nucleic acid-based molecules from PLGA microparticles and stearic acid nanoparticles

G Grassi[1,2]
N Coceani[3]
R Farra[1]
B Dapas[1]
G Racchi[2]
N Fiotti[1]
A Pascotto[4]
B Rehimers[4]
G Guarnieri[1]
M Grassi[5]

[1]Department of Internal Medicine, University Hospital of Trieste, Italy; [2]Department of Molecular Pathology, University Hospital of Tübingen, Tübingen, Germany; [3]Department of Biochemistry, Biophysics and Macromolecular Chemistry, University of Trieste, Italy; [4]Cardiovascular Department, Civic Hospital, Venezia, Italy; [5]Department of Chemical Engineering, DICAMP, University of Trieste, Italy

Correspondence: Mario Grassi
Department of Chemical, Environmental and Raw Materials Engineering, DICAMP, Piazzale Europa 1, 1 - 34127, Trieste, Italy
Tel +39 040 558 3435
Fax +39 040 569823
Email mariog@dicamp.univ.trieste.it

Abstract: We studied the mechanism governing the delivery of nucleic acid-based drugs (NABD) from microparticles and nanoparticles in zero shear conditions, a situation occurring in applications such as in situ delivery to organ parenchyma. The delivery of a NABD molecule from poly(DL-lactide-co-glycolide) (PLGA) microparticles and stearic acid (SA) nanoparticles was studied using an experimental apparatus comprising a donor chamber separated from the receiver chamber by a synthetic membrane. A possible toxic effect on cell biology, as evaluated by studying cell proliferation, was also conducted for just PLGA microparticles. A mathematical model based on the hypothesis that NABD release from particles is due to particle erosion was used to interpret experimental release data. Despite zero shear conditions imposed in the donor chamber, particle erosion was the leading mechanism for NABD release from both PLGA microparticles and SA nanoparticles. PLGA microparticle erosion speed is one order of magnitude higher than that of competing SA nanoparticles. Finally, no deleterious effects of PLGA microparticles on cell proliferation were detected. Thus, the data here reported can help optimize the delivery systems aimed at release of NABD from micro- and nanoparticles.
Keywords: nucleic acids delivery, microparticle, nanoparticle, erosion, modeling

Introduction

Nucleic acid-based drugs (NABD) represent a novel group of molecules with the potential to treat several different human diseases (Grassi et al 2004; Heidenreich 2004). Because all are constituted by either RNA, such as small interfering RNAs (Hannon and Rossi 2004) or DNA, such as DNA enzymes (Breaker 1997), NABD are rapidly destroyed in physiological fluids. Additionally, their hydrophilic nature makes cellular internalization a problematic step. Thus, to be effective in vivo, they need to be protected against degradation and the crossing of cellular membrane improved. A strategy to accomplish these requirements deals with the incorporation of NABD in microparticles made up of synthetic polymers (Jong et al 1997; Luo et al 1999; Wang et al 1999) or in polymeric nanoparticles (Hirosue et al 2001). The use of micro- and nanodevices is dictated by the fact that the smaller the particle diameter, the easier is the NABD cellular uptake (Luo and Saltzman 2000).

The mechanisms of NABD release from micro- or nanoparticles can be predicted to play a relevant role in the effectiveness of the delivery system. Thus, an investigation conducted both from the theoretical and experimental point of view in this sense is of potential relevance. Among others, a hydrodynamic condition corresponding to a virtual zero shear condition can be of interest for different applications such as trans-dermal delivery and the in situ delivery to organ parenchyma. The zero shear condition is realized when a particle suspension is put in contact with the surface of interest and no mixing is imposed on the suspension. For this purpose, we have used an experimental apparatus made up of a donor chamber separated from the receiver chamber by a

synthetic membrane. The donor chamber hosts an unstirred particle suspension while the receiver chamber hosts a pure fluid undergoing proper mixing. A mathematical model based on the hypothesis that NABD release from particles is due to particle erosion is used to interpret experimental data. This experimental set up enables the predominant mechanism governing the delivery under our conditions to be determined. In particular, in this work we focused on the study, in conditions of virtual zero shear, of the delivery kinetics of single-stranded DNA oligonucleotide, chosen as a prototype for NABD, from poly(DL-lactide-co-glycolide) (PLGA) microparticles and stearic acid (SA) nanoparticles. Additionally, for just PLGA microparticles, we explored the possible toxic effects of PLGA on cultured humans cells, evaluated by studying the effects on cell proliferation.

DNA-based molecules instead of RNA-based molecule (such as siRNAs and ribozymes) were chosed because of their better stability and lower cost.

Materials and methods

Cell culture

Human coronary smooth muscle cells (CSMC), purchased from CellSystems Biotechnologies GmbH, had no more than 9 doublings when used in the experiments. The cells were grown in a medium (defined as complete medium) containing one third Smooth Muscle Cell Basal Medium (Promocell, Heidelberg, Germany), one third Waymouth Medium MB 752/1, and one third Nutrient Mixture F12 supplemented with 15% fetal calf serum (FCS) and 1% penicillin/streptomycin (Life technologies, Gaithersburg, MD, USA). CSMCs were kept in a moist atmosphere with 5% CO_2 at 37°C.

Cell proliferation assays

2.6 mg of PLGA micro-particles were incubated with $7x10^4$ CSMC in complete growth medium for 24 hours. As control, cells treated with 12 μg of a cationic liposome commonly used to transfect CSMC (CellFectin, Invitrogen) (Grassi et al 2005) and non-treated cells were evaluated in parallel. Ten hours before harvesting, cells were pulsed with bromodeoxyuridine (BrdU) at a concentration of 10 μM. Afterwards, cells were prepared for BrdU staining as follows. Cells were trypsinized and resuspended in 100 μL of ice cold 70% ETOH for 20 min. After washing with PBS containing 0.5% bovine serum albumin (BSA), cells were treated with 2M HCl and 0.5% BSA for 20 min. After a further washing step, cells were resuspended in 0.1 M sodium borate pH 8.5 for 2 min and washed again. From each sample, an aliquot was withdrawn and incubated with 6 μL of R-phycoerythrin conjugated mouse IgG1 isotype control (PharMingen International) for 20 min. The remaining part of each sample was incubated with 6 μL of R-phycoerythrin conjugated anti-BrdU monoclonal mouse antibody (PharMingen International) for 20 min. After a final washing step, cells were resuspended in PBS containing 0.5% BSA and, for cell cycle analysis only, 8 μL of 7-Amino-Actinomycin D (Via-PROBE, Becton Dickinson). Samples were analyzed by flow cytometry (FACScalibur, Becton Dickinson) using the CellQuest software.

DNA oligonucleotide synthesis

The DNA oligonucletide used was chemically synthesized (Eurogentec, Herstal Belgium) with a length of 38 nts (GGAUCAGG CUGAUGAGUCCGUGAGGACGAA AGCAGGGG 3'), resembling the sequence of a ribozyme proved by us (Grassi et al 2005) to be effective in cultured CSMC.

Microparticle preparation

Microparticles were prepared according to the double emulsion evaporation method proposed by Nihant et al (1994). Primary emulsion was realized by mixing (high shear mixer; Silverson, UK) 1 cm^3 of phosphate buffer solution at pH 7.4 (PBS: Na_2HPO_4 4.76 g; KH_2PO_4 0.38 g; NaCl 16 g into 2 L of deionized water) containing 1000 μg of single-stranded DNA oligonucleotide, with 5 g of PLGA (Boehringer Ingelheim) solution in methylene chloride (MC; BDH Italy, Milano) and a stabilizing agent as Poloxamer F68 (Pluronc F68, BASF, Germany) (solution composition: PLGA 9% w/w, MC 90% w/w, PF68 1% w/w). Secondary emulsion was obtained by dispersing the primary emulsion, under stirring (6 blades impeller at 700 rpm) and sonication for 30 min, into a 100 cm^3 of a 2.5% w/v polyvinyl alcohol aqueous solution (PVA, Sigma, St Louis, USA). Temperature was firstly maintained at 0°C for half an hour, then increased to up to 20°C and kept constant for 2 hours in order to allow solvent (MC) removal. Microparticles were finally collected by centrifugation/filtration (0.2 μm regenerated cellulose membrane Sartorius®, Germany), washed with water, and dried under vacuum at 25°C. Theoretical single-stranded DNA oligonucleotide concentration in dry microparticles was 2000 μg/cm^3. Microparticle diameter was measured according to photon correlation spectroscopy (PCS N4Plus Beckman-Coultar; Fullerton, CA, USA) and SEM pictures were taken with EVO 40 microscope (LEO, Cambridge, UK) to confirm these results.

Nanoparticle preparation

Nanoparticle preparation was based on the formation of an oil-in-water (O/W) microemulsion. O/W microemulsions were prepared by mixing 300 mg of lipid blend components stearic acid (BDH, UK)/Labrafil® CS2125 (glycerol oleate-linoleate PEG 6 complex; Gatefossé, France) (weight ratio 95:5) with 100 mg of surfactant (sodium taurodeoxycholate acid; Sigma). 1 cm^3 of deionized water plus 0.1 cm^3 of cosurfactant (N-Buthanol BDH-UK) and 1000 μg of single-stranded DNA oligonucleotide constituted the aqueous phase that was added to the oil phase. 0.4 cm^3 of non-ionic surfactant (Tween® 80; Sigma) were added to the emulsion until the formation of a transparent, homogeneous system. All components and the microemulsion preparation were maintained at temperatures above the melting point of the lipid phase (65–70°C). Microemulsion was subsequently dispersed (dilution 1:50) in cold deionized water for 30 min and then at 20°C for 1 hour. Microemulsion stirring was ensured by a 6-blade impeller at 500 rpm. Samples of suspended nanoparticles were then washed 3 times by tangenzial flow ultrafiltration (Minitan-S Ultrafiltration System; Millipore, USA) to eliminate surfactant and cosurfactant residual. Then, dry nanoparticles were collected by lyophilization and stored at 4°C. The theoretical single-stranded DNA oligonucleotide concentration in dry nanoparticles was 2500 μg/cm^3. Nanoparticle diameter was measured using particle size analyzer (photon correlation spectroscopy PCS) and SEM microscopy in order to confirm the results.

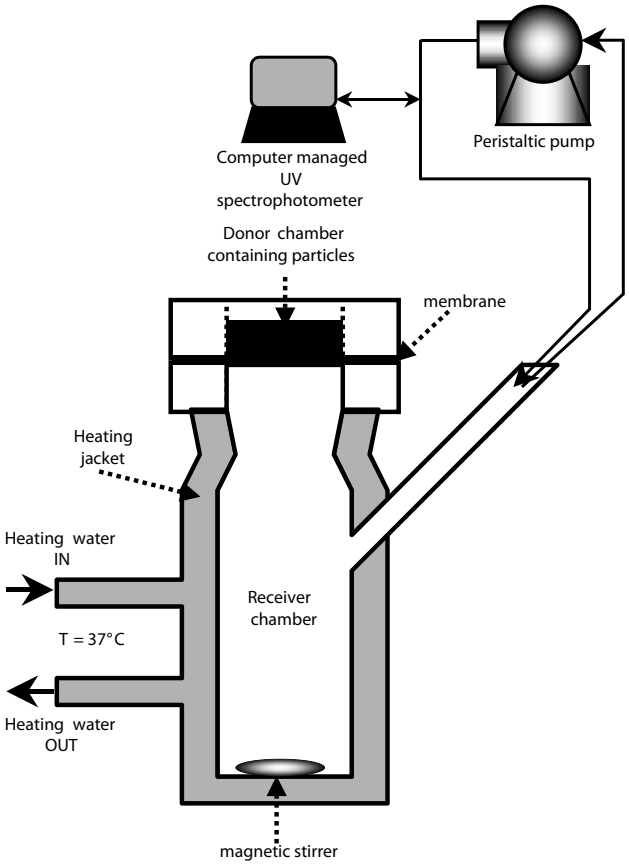

Figure 1 Schematic representation of the experimental apparatus used for release experiments (Franz cell apparatus). The synthetic membrane separates the donor chamber (not mixed) from the receiver chamber where mixing is ensured by a magnetic stirrer.

Release experiments

All release experiments were done in the Franz cell depicted in Figure 1. Basically, the cell is a double-walled beaker characterized by a top donor chamber (5 cm^3) separated from the receiver chamber (22 cm^3) by a synthetic membrane (polysulphon, 10^4 cut off, Millipore). Lower and higher membrane cut off was discharged, as lower cut off implied a lower membrane permeability reflecting very long release experiments. On the contrary, higher cut off membranes also allowed the permeation of part of the materials constituting our particles and this caused some interference problems in the UV determination of DNA concentration.

Although the donor chamber was not mixed, a magnetic stirrer ensured receiver chamber mixing (500 rpm). System thermostatic conditions (37°C) were ensured by means of a heating jacket (see Figure 1). Single-stranded DNA oligonucleotide concentration in the receiver chamber was monitored via an on-line computer-managed Perkin Elmer Lambda Series UV spectrophotometer (wavelength λ = 255 nm, cell path = 1 cm). A peristaltic pump was used for system liquid circulation (28 cm^3/min). In this experimental set up single-stranded DNA oligonucleotide loaded particles experienced virtually zero shear conditions during release. Three different kinds of release experiments were performed. In the first kind, the donor chamber was filled by 4 cm^3 of a PBS solution at pH 7.4 characterized by a single-stranded DNA oligonucleotide concentration equal to 10 μg/cm^3, while the receiver chamber contained 22 cm^3 of a PBS solution at pH 7.4. This experimental configuration served to estimate single-stranded DNA oligonucleotide diffusion coefficient through the polysulphon membrane. In the other two kinds of release experiments, the donor chamber was filled by 5 cm^3 buffer pH 7.4 solution containing 100 mg of particles. The receiver chamber always contained 22 cm^3 of PBS solution pH 7.4. These tests served to the evaluation of particle erosion speed. All release tests were performed in duplicate and the experimental standard error never exceeded 15% of experimental mean.

Modeling

In the light of the programmed experimental tests, 2 mathematical models need to be examined. The first refers to single-stranded DNA oligonucleotide permeation across the synthetic membrane assuming that the donor chamber contains a single-stranded DNA oligonucleotide PBS solution of known initial concentration. The second refers to the simultaneous single-stranded DNA oligonucleotide release from particles and permeation across the synthetic membrane.

Assuming that the synthetic membrane thickness is very small, it follows that a linear concentration profile of the single-stranded DNA oligonucleotide always holds inside the membrane (Grassi and Colombo 1999). In addition, we assume that no interactions between single-stranded DNA oligonucleotide and synthetic membrane occur (Coviello et al 2005; Grassi and Grassi 2005). Thus, the single-stranded DNA oligonucleotide concentration in the receiver chamber C_r can be evaluated according to the following equations:

$$V_r \frac{dC_r}{dt} = \frac{SD}{L_M}\left(k_d C_d - k_r C_r\right) \quad (1)$$

$$V_d C_d + S\int_0^{L_M} C_M(X)dX + V_r C_r = V_d C_{d0} \quad (2)$$

where C_r, V_r, and C_d, V_d are, respectively, single-stranded DNA oligonucleotide concentration and volume of the receiver and donor chamber, t is time, S and L_M are, respectively, membrane surface and thickness, k_d and k_r are, respectively, single-stranded DNA oligonucleotide partition coefficients on the donor and receiver chamber side, C_{d0} is the initial single-stranded DNA oligonucleotide concentration in the donor chamber, X is the abscissa, and D is the single-stranded DNA oligonucleotide diffusion coefficient in the membrane. Eq.(1) is a kinetic equation stating that the time variation of the single-stranded DNA oligonucleotide mass (V_rC_r) in the receiver solution depends on the concentration gradient ($k_dC_d - k_rC_r)/L_M$), the diffusion coefficient (D), and the membrane area (S) available for permeation. Eq.(2), instead, is a mass balance stating that, at any time t, the sum of the single-stranded DNA oligonucleotide mass present in the donor chamber (V_dC_d), in the membrane ($S\int_0^{L_M} C_M(X)dX$) and in the receiver chamber (V_rC_r) must be equal to the initial ($t = 0$) single-stranded DNA oligonucleotide mass present in the donor chamber when both the membrane and the receiver chamber are empty of single-stranded DNA oligonucleotide. Assuming that the initial single-stranded DNA oligonucleotide concentration in the donor chamber is C_{d0}, that a linear single-stranded DNA oligonucleotide concentration profile in the membrane holds, and expressing C_d as a function of C_r by m s of eq.(2), eq.(1), the model solution is:

$$C_r(t) = \frac{k_d C_{d0} V_d}{k_d V_r + k_r V_d + SL_M k_r k_d}\left(1 - e^{\left(\frac{-S\delta t}{V_r}\right)}\right) \quad (3)$$

$$\delta = \frac{D}{L_M}\left(k_r + k_d \frac{V_r + 0.5 S L_M k_r}{V_d + 0.5 S L_M k_d}\right) \quad (3')$$

Eq.(3) represents the analytical expression of the first model.

Although the real physical situation can be more complicated by the fact that single-stranded DNA oligonucleotide molecules can be in part inside the particles and, in part, adsorbed on to particle surfaces (particularly true for nanoparticles), the main hypotheses of the second model rely on the assumption that all particles are characterized by the same initial mean radius R_0 and that single-stranded DNA oligonucleotide release from particles occurs according to a pure particle erosion mechanism. In particular, we assume that particle radius R declines according to a linear law:

$$R(t) = R_0 - bt \quad (4)$$

where b is the erosion velocity. Accordingly, if the hypotheses of model 1 are always true (thin membrane and no single-stranded DNA oligonucleotide interaction with the membrane), the second model differential equations are:

$$V_d \frac{dC_d}{dt} = C_{p0}\frac{dV_p}{dt} - \frac{SD}{L_M}\left(k_d C_d - k_r C_r\right) \quad (5)$$

$$\frac{dV_p}{dt} = N_p \frac{d}{dt}\left(\frac{4}{3}\left(R_0^3 - R^3(t)\right)\right) = -N_p 4\ R^2(t)\frac{dR(t)}{dt} = N_p 4\ R^2(t)b \quad (6)$$

$$V_d C_d + V_r C_r + N_p \frac{4}{3}\ C_{p0} R^3(t) + S\int_0^{L_M} C_M(X)dX \quad N_p \frac{4}{3}\ C_{p0} R_0^3 \quad (7)$$

where C_{p0} is single-stranded DNA oligonucleotide concentration in the particles and V_p is the eroded volume of the N_p particles present in the donor chamber. Eq.(5) is a kinetics equation stating that the time variation of single-stranded DNA oligonucleotide mass in the donor chamber (V_dC_d) is determined by the single-stranded DNA oligonucleotide income due to particle erosion ($C_{p0}\frac{dV_p}{dt}$) less the amount

of diffusion through the membrane ($\frac{SD}{L_M}(k_dC_d - k_rC_r)$). Eq.(6), another kinetics equation, models the increase of the eroded volume and it states that it depends on the square of particles radius and, consequently (see also eq.(4)), on the square of time. Finally, eq.(7) is the new expression of the single-stranded DNA oligonucleotide mass balance that differs from the previous one (eq.(2)) only for the presence of particles. Indeed, an additional term ($N_p\frac{4}{3}\pi C_{p0}R^3(t)$) related to the amount of single-stranded DNA oligonucleotide still present inside the particles at time, t, appears in eq.(7), left hand side. Finally, the total amount of single-stranded DNA oligonucleotide must be always equal to the amount initially present inside the particles ($N_p\frac{4}{3}\pi C_{p0}R_0^3(t)$). Eqs.(5)–(7) solution, assuming that $C_r = C_d = 0$ at the beginning ($t = 0$), yields the following analytical solution:

$$C_d(t) = Z_1 + Z_2(R_0 - bt) + Z_3(R_0 - bt)^2 + Z_4(R_0 - bt)^3 + Z_5e^{(-At)} \quad (8)$$

$$C_r(t) = \alpha - \beta C_d(t) - \gamma(R_0 - bt)^3 \quad (9)$$

where Z_1, Z_2, Z_3, Z_4, Z_5, α, β, and γ are time-independent parameters depending on system geometry, initial conditions erosion kinetics parameter, and single-stranded DNA oligonucleotide diffusion coefficient in the membrane (see Appendix for a detailed expression of these parameters). Obviously, this second model expression holds until particles are not completely eroded ($R(t) \geq 0$). Indeed just after particle disappearance (it occurs when $R = 0$; $t^* = R_0/b$), the second model expression becomes:

$$V_r\frac{dC_r}{dt} = \frac{SD}{L_M}(k_dC_d - k_rC_r) \quad (10)$$

$$V_dC_d + V_rC_r + S\int_0^{L_M} C_M(X)dX = N_p\frac{4}{3}\pi C_{p0}R_0^3 \quad (11)$$

Indeed, for $t > t^*$, the second model identifies with the first model as the erosion phenomenon disappears. The eqs.(10)–(11) solution, assuming that for $t = t^*$
$C_r(t^*) = \alpha - \beta C_d(t) - \gamma(R_0 - bt^*)^3 = C^*$ (see eq.(9)), reads:

$$C_r(t) = \frac{\beta_1}{\gamma_1} + (C^* - \frac{\beta_1}{\gamma_1})\, e^{(-\alpha_1\gamma_1(t-t^*))} \quad (12)$$

where, again, α_1, β_1, and γ_1 are time-independent parameters depending on system geometry, initial conditions, erosion kinetics parameter, and single-stranded DNA oligonucleotide diffusion coefficient in the membrane (see Appendix for a detailed expression of these parameters).

Results and discussion

Figure 2a reveals that PLGA microparticles are characterized by a perfect spherical shape and that diameter ranges between 12 μm and 2 μm (mean 7–8 μm), confirmed by photon correlation spectroscopy (PCS). On the contrary, Figure 2b reveals that SA nanoparticles have an ellipsoidal shape, the smaller diameter (~300 nm) being approximately half the longer one (~600 nm). PCS measurements gave a mean nanoparticle spherical diameter of 280 nm. Notably, the nanoparticle size distribution is much more narrow than that for microparticles.

Before studying the release properties of the micro- and nanoparticle preparation loaded with single-stranded DNA oligonucleotides, we wanted to make sure that the polymers used do not significantly affect human cell viability. For this

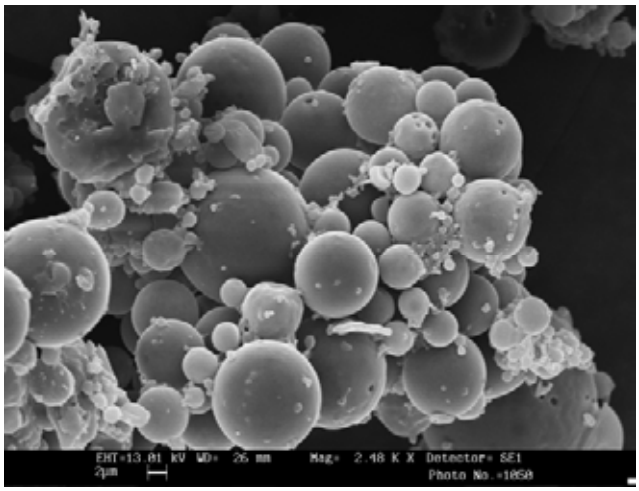

Figure 2a SEM image of poly(DL-lactide-co-glycolide) (PLGA) microparticles. They are spherical particles of diameter ranging between approximately 8 μm and 2 μm.

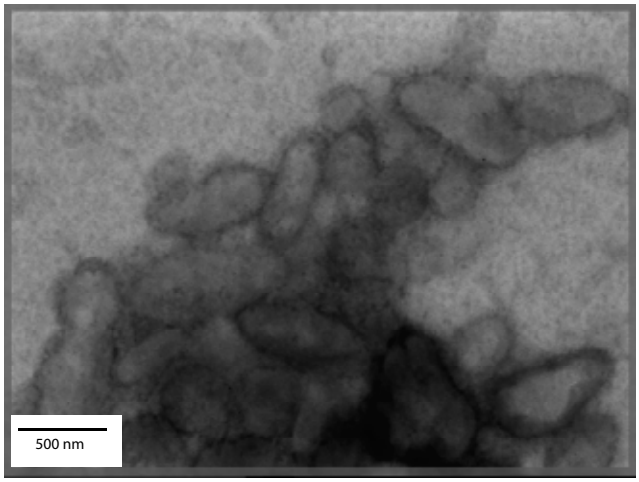

Figure 2b SEM image of stearic acid (SA) nanoparticles. They are ellipsoidal, with the larger diameter (~600 nm) 2 times the smaller one (~300 nm).

purpose, the effects on cell proliferation, a sensible marker of cell viability, were explored. Whereas studies dealing with SA effect on cell biology have been already reported (Lima et al 2002), the effect of the combination of chemicals we used to prepare the PLGA microparticles is less clear. For this reason, we limited the analysis to the effect on cell proliferation of PLGA microparticles. As target cells we used human CSMC, known to be implicated in vascular pathologies (Grassi et al 2005), which can benefit from the release of NABD by means of micro- and nanoparticles loaded with therapeutic molecules (Labhasetwar et al 1997). The double staining technique used (Dolbeare et al 1983; Grassi et al 2005) allows detection of cells in the different phases of the cell cycle as reported in the representative experiment of Figure 3 and summarized in Figure 4. It is evident that there are no significant differences in cell cycle phase distribution in cells treated by PLGA nanoparticles compared with controls cells represented by cells treated by a liposome commonly used to transfect CSMC and non-treated cells. We thus concluded that, limited to this fundamental biological parameter, PLGA microparticles do not substantially affect cell viability. It should be also added that light microscopy inspection of the cells in the different treatments did not reveal any significant difference in morphology, further strengthening the concept of the compatibility of PLGA microparticles we prepared with CSMC biology (data not shown).

We then moved to the evaluation of the release properties of the micro- and nanoparticle preparations loaded with the single-stranded DNA oligonucleotide, chosen as a prototype of NABD. Figure 5, referring to single-stranded DNA oligonucleotide permeation, shows the very good agreement between experimental data (symbols) and first model (eq.(3)) best fit (solid line). This evidence is also statistically proved by the huge value assumed by the F value (Draper and Smith 1966) ($F = 53293 >> F_{TABULATED}(\nu_1 = 1, \nu_2 = 87, 0.01) = 6.9$). This means that first model hypotheses (thin membrane and no plasmid DNA/membrane interactions) are reasonable. Model fitting, performed assuming unitary values for both the partition coefficients k_d and k_r, yields the following value for the single-stranded DNA oligonucleotide diffusion coefficient in the membrane: $D = (7.5 \pm 0.1)*10^{-8}$ cm^2/s. Figure 6 reports the second model (eqs.(9) and (12)) best fit (solid line) on experimental data (symbols) referring to single-stranded DNA oligonucleotide release from PLGA microparticles and subsequent permeation through the membrane. Also in this case the data fitting is good, as also proved by the huge F value ($F = 10555 >> F_{TABULATED}(\nu_1 = 1, \nu_2 = 69, 0.01) = 6.9$). In order to get a more reliable evaluation of the model fitting

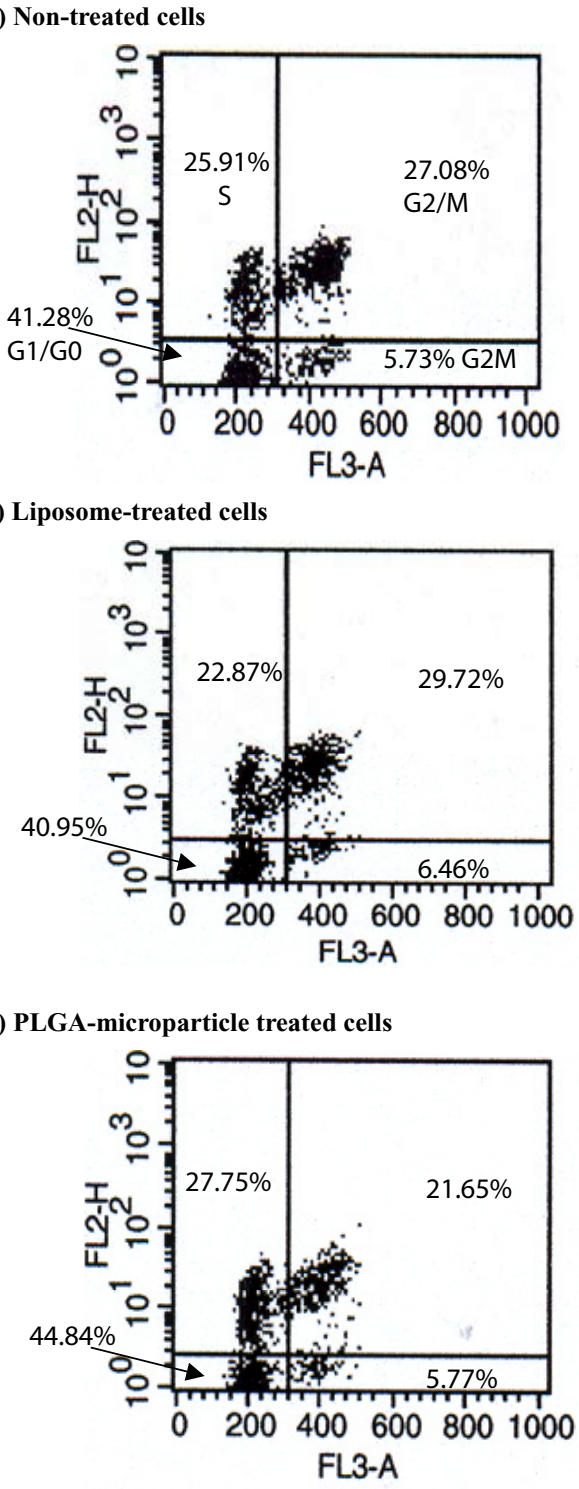

Figure 3 Cell cycle phase distribution. Cell cycle phase distribution was evaluated for non-treated human coronary smooth muscle cells (CSMC) (A), CSMC treated by a commonly used transfection reagent (B), and poly(DL-lactide-co-glycolide) (PLGA) microparticles (C). Cell cycle phase distribution was performed by a DNA double staining DNA procedure which enables determination of the amount of total DNA/per cell (reported on the abscissa as FL3-A) and the amount of newly synthesized DNA (reported on the ordinates as FL2-H). Based on these measurement it is possible to calculate the amount of cells in the different phases of the cell cycle as reported in each panel. G1/G0 = cells in the initial phase of cell cycle; S = cells synthesizing new DNA; G2-M = cells in the process of division (cytokinesis). No substantial differences were detected among the different treatments.

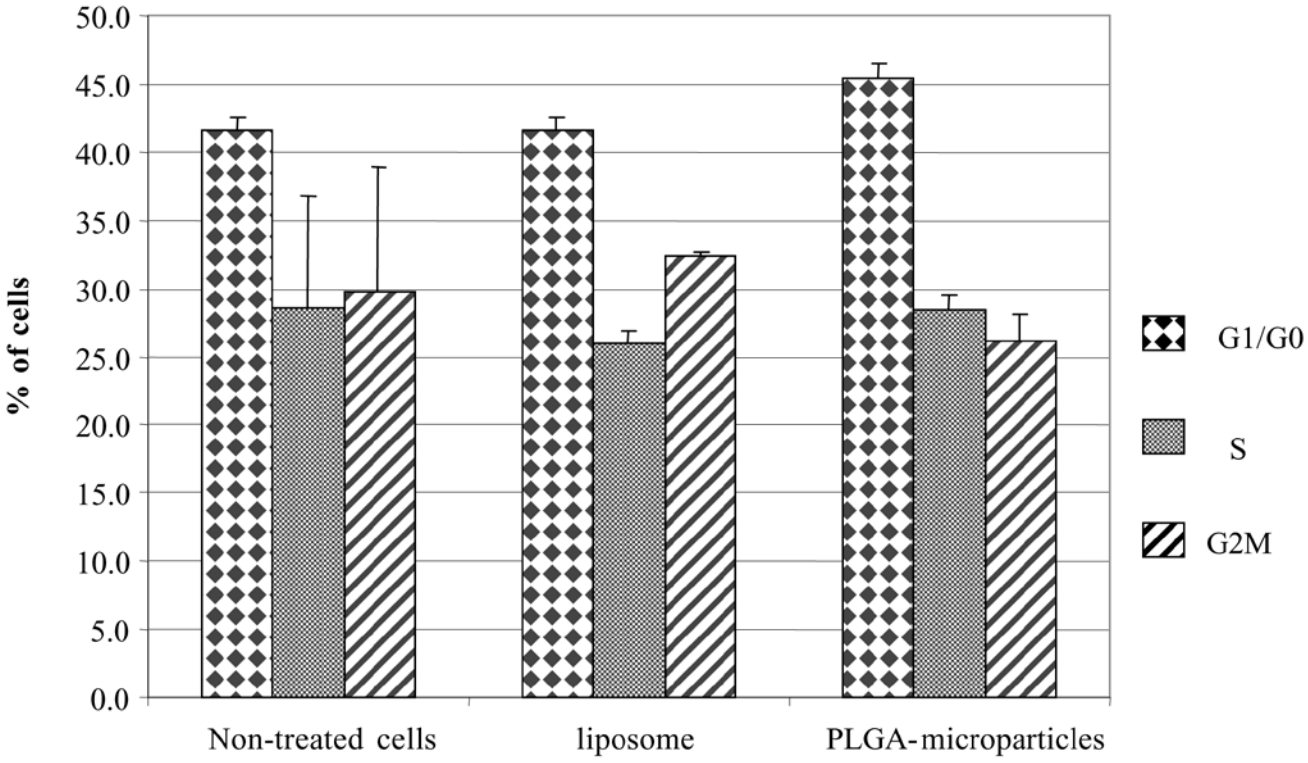

Figure 4 Summarized cell cycle phase distribution data. Cell cycle phase distribution was evaluated for non-treated cells human coronary smooth muscle cells (CSMC), CSMC treated by a commonly used transfection reagent (liposome), and poly(DL-lactide-co-glycolide) (PLGA) microparticles. Data are reported as means ± SD (n=3). No statistically significant differences were noted among the different treatments.

parameters (D and b), the initial D value is assumed equal to that previously determined in the single-stranded DNA oligonucleotide permeation experiment (($(7.5 \pm 0.1)*10^{-8}$ cm^2/s)) as, in our hypotheses, D should not be influenced by the erosion phenomenon taking place in the donor chamber. Additionally, the initial b value is deduced on the basis of the data shown in Figure 7. This figure shows the reduction in mean PLGA microparticle diameter in PBS, 37°C, in zero shear conditions (evaluated by PCS). Although the reduction is not exactly linear, rough b estimation can be performed by calculating the ratio between radius reduction and time needed for this decrease. This leads to $b = 2*10^{-9}$ cm/s. On

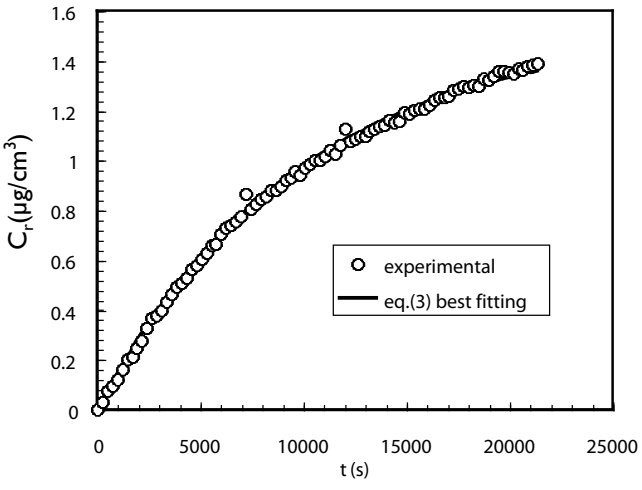

Figure 5 Comparison between experimental data (open circles) referring to single-stranded DNA oligonucleotides permeation through the synthetic membrane and model best fitting (eq.(3), solid line). C_r indicates single stranded DNA oligonucleotide concentration in the receiver chamber.

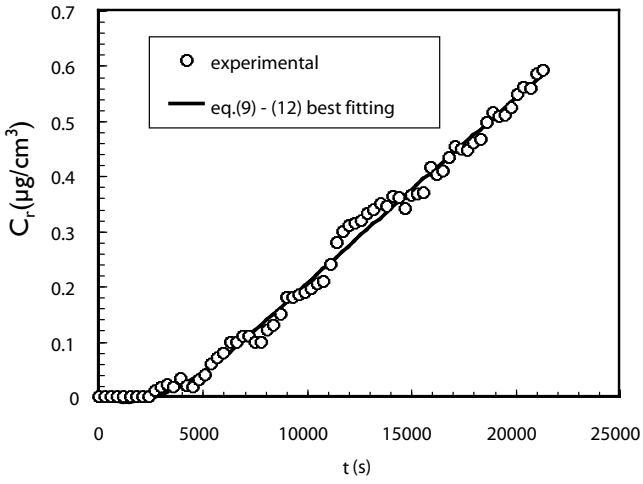

Figure 6 Comparison between experimental data (open circles) referring to single-stranded DNA oligonucleotides release from poly(DL-lactide-co-glycolide) (PLGA) microparticles and subsequent permeation through the synthetic membrane and model best fitting (eq.(9) – (12), solid line). C_r indicates single-stranded DNA oligonucleotide concentration in the receiver chamber.

the basis of these values, model data fitting yields $D = (1.0 \pm 0.05)*10^{-7}$ cm^2/s and $b = (3.6 \pm 0.3)\ 10^{-8}$ cm/s. Although statistically different, this value for the single-stranded DNA oligonucleotide diffusion coefficient is close to that previously determined, as the difference is below 30%. On the contrary, a one order of magnitude difference exists between b value evaluated according to second model best fit and that estimated on the basis of PLGA microparticle erosion (see Figure 7). Nevertheless, due to the difficulty of exactly re-creating the same hydrodynamic conditions in both cases, we can accept this discrepancy. It is worth mentioning that, according to this data fitting, complete particle erosion takes 10 555 s (= t^*) and this corresponds to single-stranded DNA oligonucleotide concentration in the receiver environment equal to approximately 0.22 μg/cm^3. This means that up to 10 555 s, eq.(9) holds, then eq.(12) holds. Qualitative experimental observations verified that after around 10 000 s, particle volume was greatly reduced although complete particle disappearance did not occur. This discrepancy with model prediction can be explained by remembering that our model assumes all particles were equal (same diameter) and perfectly spherical. If microparticles are really spherical, they do not constitute a perfect mono-disperse particles ensemble as shown in Figure 2a. Bigger particles require more time for complete dissolution.

In fitting single-stranded DNA oligonucleotide release from SA nanoparticles and subsequent permeation, initial D value was fixed to $(7.5 \pm 0.1)*10^{-8}$ cm^2/s and initial b value was assumed to be $2*10^{-9}$ cm/s, as we did in the PLGA microparticles case. Indeed, theoretically, D should be the same in all the release tests performed. Unfortunately, as nanoparticle dimensions prevented a reliable experimental b determination, unlike microparticles, we decided to assume the value for microparticle erosion. Figure 8 clearly shows that in this case data fitting is more than satisfactory and this assumption is statistically supported by the huge F value ($F = 31647 >> F_{TABULATED}(\nu_1 = 1, \nu_2 = 87, 0.01) = 6.9$). Fitting parameters gave $D = (1.5 \pm 0.1)*10^{-7}$ cm^2/s and $b = (2.8 \pm 0.2)x10^{-9}$ cm/s. Also, in this case the single-stranded DNA oligonucleotide diffusion coefficient is bigger (two fold) than that evaluated in the permeation experiment and that evaluated in the microparticle erosion/permeation experiment (exceeded by 50%). This evidence let us conclude that the single-stranded DNA oligonucleotide diffusion coefficient in our synthetic membrane is around 10^{-7} cm^2/s. In addition, data fitting reveals that the SA nanoparticle erosion is one order of magnitude smaller than that found for PLGA microparticles. Thus, theoretically, SA nanoparticles disappear after 5360 s (= t^*) and, consequently, eq.(9) holds at up to 5360 s, and then eq.(12) holds. Also in this case, qualitative experimental observations verified that after around 5000 s, particle volume was greatly reduced although a complete particle disappearance did not occur. This discrepancy with model prediction can be explained by remembering that our nanoparticles are not perfectly spherical (see Figure 2b), as required by the model.

The fact that nanoparticle erosion is smaller than that of microparticle erosion could be relevant in the optimization of NABD delivery from micro- and nanoparticles. Indeed, in relation to a particular pathology, the desired NABD release

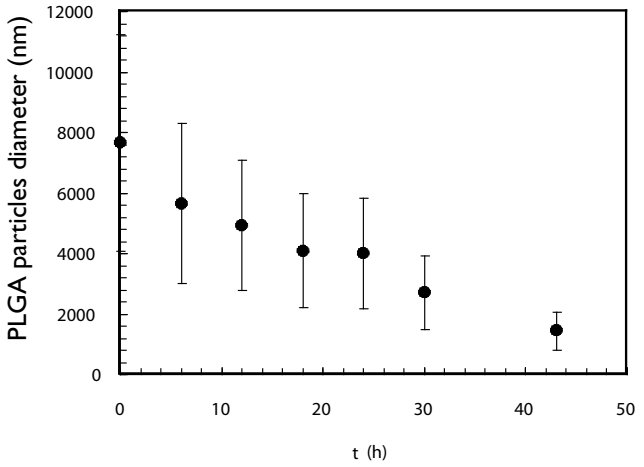

Figure 7 poly(DL-lactide-co-glycolide) (PLGA) microparticle diameter decrease in zero shear conditions (PBS, 37°C). Measures were performed by photon correlation spectroscopy.

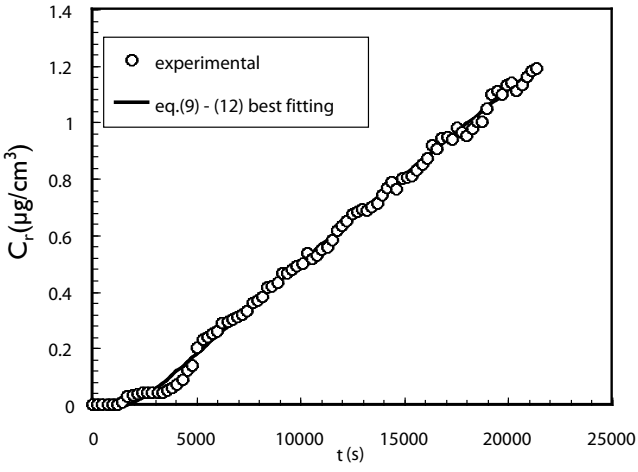

Figure 8 Comparison between experimental data (open circles) referring to single stranded DNA oligonucleotides release from SA nanoparticles and subsequent permeation through the synthetic membrane and model best fitting (eq.(9) – (12), solid line). C_r indicates single-stranded DNA oligonucleotide concentration in the receiver chamber.

rate can be reached by properly selecting particle dimensions (size distribution) and composition.

Conclusions

In this paper we developed an experimental and theoretical approach to clarify how NABD can be released from PLGA microparticles and SA nanoparticles in zero shear conditions. This situation can be experienced in some delivery situations such as those found in trans-dermal release and the in situ release to organ parenchyma. Attention was focused on the evaluation of the possible toxic effects on cell biology for only PLGA microparticles, as investigations already exist for the effects of SA on cell biology (Lima et al 2002). For NABD release from PLGA microparticles and SA nanoparticles, experimental evidence and the theoretical interpretation of the data lead to the conclusion that NABD release from PLGA microparticles and SA nanoparticles in zero shear conditions is perfectly compatible with a pure particle erosion mechanism. In addition, the release kinetics strongly depend on the material constituting the particles. We also found that PLGA microparticle erosion is, approximately, one order of magnitude higher than that for SA nanoparticles. These data suggest that a proper balance between small and big particles, eventually of different materials, can be used to obtain the delivery kinetics suitable for the specific application. Finally, for evaluating the possible toxic effects of PLGA microparticles on cell biology, we could not show any detectable negative effects, at least on cell proliferation and cell morphology, two pivotal biological parameters.

In conclusion, we believe that the reported observations can help optimize delivery systems aimed at release of NABD from micro- and nanoparticles, which have applications in many in situ delivery conditions.

Acknowledgments

This work was supported in part by the Dr. Karl-Kuhn-award 2003, by the Fondazione Cassa di Risparmio of Trieste, by Fondazione Sostegno delle Strutture Cardiovascolari, by the Fondazione Casali of Trieste and by Fondo Trieste 2006. G Grassi is supported by the program Rientro cervelli art. 1 DM n.13, MIUR (Ministero dell'Istruzione, dell'Università e della Ricerca Scientifica).

References

Breaker RR. 1997. DNA enzymes. *Nat Biotechnol,* 15:427-31.

Coviello T, Alhaique F, Parisi C, et al. 2005. A new polysaccharidic gel matrix for drug delivery: preparation and mechanical properties. *J Control Release*, 102:643-56.

Dolbeare F, Gratzner H, Pallavicini MG, Gray JW. 1983. Flow cytometric measurement of total DNA content and incorporated bromodeoxyuridine. *Proc Natl Acad Sci U S A*, 80:5573-7.

Draper N, Smith H. 1966. Applied regression analysis. New York: John Wiley & Sons, Inc.

Grassi G, Schneider A, Engel S, et al. 2005. Hammerhead ribozymes targeted against cyclin E and E2F1 co-operate to down regulate coronary smooth muscle cells proliferation. *J Gene Med*, 7:1223-34.

Grassi M, Grassi G. 2005. Mathematical modelling and controlled drug delivery: matrix systems. *Curr Drug Deliv*, 2:97-116.

Grassi G, Dawson P, Guarnieri G, et al. 2004. Therapeutic potential of hammerhead ribozymes in the treatment of hyper-proliferative diseases. *Curr Pharm Biotechnol*, 5:369-386.

Grassi M, Colombo I. 1999. Mathematical modelling of drug permeation through a swollen membrane. *J Control Release*, 59:343-359.

Hannon GJ, Rossi JJ. 2004. Unlocking the potential of the human genome with RNA interference. *Nature*, 431:371-8.

Heidenreich O. 2004. Oncogene suppression by small interfering RNAs. *Curr Pharm Biotechnol*, 5:349-54.

Hirosue S, Muller BG, Mulligan RC, Langer R. 2001. Plasmid DNA encapsulation and release from solvent diffusion nanospheres. *J Control Release*, 70:231-42.

Jong YS, Jacob JS, Yip KP, et al. 1997. Controlled release of plasmid DNA. *J Control Release*, 47:123-34.

Labhasetwar V, Song C, Levy R. 1997. Nanoparticles drug delivery system for restenosis. *Adv Drug Del Rev*, 24:63-85.

Lima TM, Kanunfre CC, Pompéia C, et al. 2002. Ranking the toxicity of fatty acids on Jurkat and Raji cells by flow cytometric analysis. *Toxicol in Vitro*, 16:741-7.

Luo D, Woodrow-Mumford K, Belcheva N, et al. 1999. Controlled DNA delivery systems. *Pharm Res*, 16:1300-8.

Luo D, Saltzman WM. Synthetic DNA delivery systems. 2000. *Nature Biotechnol*, 18:33-7.

Nihant N, Schugens C, Grandfils C, et al. 1994. Polylactide microparticles prepared by double emulsion/evaporation technique. I. Effect of primary emulsion stability. *Pharm Res*, 11:1479-84.

Wang D, Robinson DR, Kwon GS, Samuel J. 1999. Encapsulation of plasmid DNA in biodegradable poly(D,L-lactic-co-glycolic acid) microspheres as a novel approach for immuno-gene delivery. *J Control Release*, 57:9-18.

Appendix

Assuming that a linear concentration profile instantaneously develops inside the membrane, the integral appearing in eq.(7) becomes:

$$\int_0^{L_M} C_M(X)\mathrm{d}X = \int_0^{L_M}\left(C_d k_d - \frac{C_d k_d - C_r k_r}{L_M} X\right)\mathrm{d}X = \frac{L_M}{2}\left(C_d k_d + C_r k_r\right) \tag{13}$$

Accordingly, eq.(7) can be used to express C_r in function of $R(t)$ and $C_d(t)$:

$$C_r = \alpha - \beta C_d(t) - \gamma\left(R(t)\right)^3 \tag{14}$$

where:

$$\alpha = \frac{N_p \frac{4}{3}\pi C_{p0} R_0^3}{V_r + 0.5 S L_M k_r} \qquad \beta = \frac{V_d + 0.5 S L_M k_d}{V_r + 0.5 S L_M k_r} \qquad \gamma = \frac{N_p \frac{4}{3}\pi C_{p0}}{V_r + 0.5 S L_M k_r} \tag{15}$$

Inserting eq.(14) into eq.(5) gives the following differential equation:

$$\frac{\mathrm{d}C_d}{\mathrm{d}t} + AC_d = BR^2 - ER^3 - F \tag{16}$$

where:

$$A = \frac{SD}{L_M V_d}\left(k_d + \beta k_r\right) \quad B = N_p \frac{4\pi b C_{p0}}{V_d} \qquad E = \frac{SDk_r\gamma}{L_M V_d} \qquad F = \frac{SDk_r\alpha}{L_M V_d} \tag{17}$$

Imposing that $C_d = 0$ for $t = 0$, eq.(16) solution reads:

$$C_d(t) = Z_1 + Z_2(R_0 - bt) + Z_3(R_0 - bt)^2 + Z_4(R_0 - bt)^3 + Z_5 e^{(-At)} \tag{8}$$

where:

$$Z_1 = \frac{F}{A} + \frac{2b^2}{A^3}\left(B - \frac{3bE}{A}\right) \qquad Z_2 = \frac{2b}{A^2}\left(B - \frac{3bE}{A}\right) \quad Z_3 = \frac{1}{A}\left(B - \frac{3bE}{A}\right) \tag{18}$$

$$Z_4 = -\frac{E}{A} \qquad Z_5 = \frac{ER_0^3 - F - \left(B - \frac{3bE}{A}\right)\left(R_0^2 + \frac{2bR_0}{A} + \frac{2b^2}{A^2}\right)}{A} \tag{19}$$

C_r temporal evolution is then given by eq.(9) or (14).

For $t \geq t^*$ (= R_0/b), eq.(8) and (14) no longer hold and model solution is given by solving eq.(10) and (11):

$$V_r \frac{\mathrm{d}C_r}{\mathrm{d}t} = \frac{SD}{L_M}\left(k_d C_d - k_r C_r\right) \tag{10}$$

$$V_d C_d + V_r C_r + S\int_0^{L_M} C_M(X)\mathrm{d}X = N_p \frac{4}{3}\pi C_{p0} R_0^3 \tag{11}$$

Inserting eq.(13) into eq.(10), it is possible to express C_d as a function of C_r:

$$C_d = \frac{N_p \frac{4}{3}\pi C_{p0} R_0^3}{V_d + 0.5 S L_M k_d} - \frac{V_r + 0.5 S L_M k_p}{V_d + 0.5 S L_M k_d} C_r \tag{20}$$

Inserting eq.(20) into eq.(10) leads to:

$$\frac{dC_r}{dt} = \alpha_1(\beta_1 - \gamma_1 C_r) \tag{21}$$

where:

$$\alpha_1 = \frac{DS}{L_M V_r} \qquad \beta_1 = \frac{k_d N_p \frac{4}{3}\pi C_{p0} R_0^3}{V_d + 0.5 S L_M k_d} \qquad \gamma_1 = k_d \frac{V_r + 0.5 S L_M k_p}{V_d + 0.5 S L_M k_d} \tag{22}$$

Imposing that, for $t = t^*$, $C_r = C_r^* = \alpha\text{-}\beta C_d(t^*)$, eq.(21) solution is given by eq.(12):

$$C_r(t) = \frac{\beta_1}{\gamma_1} + \left(C_r^* - \frac{\beta_1}{\gamma_1}\right) e^{(-\alpha_1\gamma_1(t-t^*))} \tag{12}$$